Int. J. Solids Structures Vol. 15, pp. 335–357
© Pergamon Press Ltd., 1979. Printed in Great Britain

0020-7683/79/0401-0335/$02.00/0

MIXTURE THEORY FOR LONGITUDINAL WAVE PROPAGATION IN UNIDIRECTIONAL COMPOSITES WITH CYLINDRICAL FIBERS OF ARBITRARY CROSS SECTION—II

COMPUTATIONAL PROCEDURE†

H. MURAKAMI‡, A. MAEWAL§ and G. A. HEGEMIER¶

Department of Applied Mechanics and Engineering Sciences, University of California, San Diego, La Jolla, CA 92093, U.S.A.

(*Received* 27 *March* 1978; *in revised form* 18 *September* 1978)

Abstract—A variational principle-based finite element procedure is described for solution of microstructure boundary value problems derived in the first part of the paper in order to calculate the mixture properties that are required in the mixture theory formulated therein. Numerical analyses are carried out for several microstructural geometries of practical interest. For circular fibers arranged in a hexagonal array, it is found that the concentric circular cylinders approximation often used in practice provides a satisfactory estimate of mixture properties. In case of rectangular fibers arranged in similar unit cells, however, the approximation is adequate for square fibers, but its accuracy decreases with increase in aspect ratio of the unit cell. Finally, the theory is used to study dispersion of longitudinal waves in composites with several microstructural geometries of practical interest.

INTRODUCTION

In the first part of this paper[1], a mixture theory was derived for propagation of longitudinal waves in unidirectional composites with cylindrical fibers of arbitrary cross section. The theory contains a number of mixture properties which are required to be evaluated from solutions of static micro-structure boundary value problems. Analytical solution of these MBVPs is not possible for most microstructural geometries of interest unless further approximations are introduced. Because of this, a variational principle-based finite element procedure is developed in the following sections for efficient solution of the MBVPs.

In the lowest order solution the asymptotically derived mixture theory allows axial displacements in the two constituents to be independent of each other and to be functions of the axial coordinate and time only. As a result, various stress and displacement quantities are discontinuous across the interface and the necessary continuity is restored by requiring that the interface conditions be satisfied by the solution composed of the two lowest order expansions. Consequently, the MBVPs, being essentially the second order problems in the asymptotic scheme, contain jumps across the interface in the derivatives of the field variables. It is this feature of the MBVPs that makes them especially interesting from both analytical and computational points of view.

In the following presentation, after a restatement of the pertinent equations from the first part for easy reference, variational principles for the MBVPs are developed. To satisfy the jump conditions across the interface, appropriate Larangian multipliers are introduced in the variational principles. Consequently, the latter exhibit some resemblance to the variational principles used in construction of hybrid finite element models, with the notable difference that in our formulation the Lagrangian multipliers are defined only along those inter-element boundaries that form the interface between the fiber and the matrix.

Based on the variational principles, triangular elements are used to discretize the MBVPs. The procedure for solution of the resulting algebraic equations is similar to the well-known substructuring technique in that all but the interface nodal variables are first eliminated from

†Research was sponsored by Air Force Office of Scientific Research.
‡Research Assistant.
§Postdoctoral Fellow. Now at: Systems, Science and Software, La Jolla, California, U.S.A.
¶Professor.

the system of equations. Once the interface quantities have been calculated, the other nodal variables are easily obtained by back-substitution.

The proposed computational scheme has been used to conduct extensive parametric studies for microstructural geometries of practical interest. For circular fibers arranged in a hexagonal array, it is found that the concentric circular cylinders approximation often used in practice provides an adequate estimate of the mixture properties. For rectangular fibers arranged in a geometrically similar array, the effect of aspect ratio of the fiber cross section is quite important. In particular, if the aspect ratio of the fiber cross section is substantially different from unity, the concentric circular cylinders approximation fails to be accurate and a numerical analysis of the type envisaged here becomes essential.

As an application of the theory, dispersion of longitudinal waves is studied to delineate the range of geometrical parameters and material properties which significantly effect the composite response.

SUMMARY OF BASIC EQUATIONS

In the following development, the same notation as introduced in the first part[1] will be utilized. All the variables are dimensionless quantities. The unit cell, bounded by a closed curve $\mathscr{C}$, contains the fiber and the matrix in the domains $A^{(1)}$ and $A^{(2)}$, respectively, separated by the interface $\mathscr{S}$. Lower case Latin indices range from 1 to 2, (x_1, x_2) being the rectangular Cartesian coordinates in the plane of the fiber cross section. As usual, repeated indices imply summation unless noted otherwise.

The basic equations of the mixture theory for the average axial displacements in the fiber and the matrix are the following:

(a) *Conservation of average axial momentum*

$$\sigma_{33}^{(1p)} - \rho^{(1p)}\ddot{u}_3^{(1a)} = -P, \tag{1a}$$

$$\sigma_{33}^{(2p)} - \rho^{(2p)}\ddot{u}_3^{(2a)} = P. \tag{1b}$$

(b) *Constitutive equations*

$$\sigma_{33}^{(\alpha p)} = (\lambda^{(\alpha p)} + 2\mu^{(\alpha p)})u_{3,3}^{(\alpha a)} - (-1)^{\alpha}K^{(\alpha)}J(x_3, t), \tag{2}$$

$$J(x_3, t) = \lambda^{(2)}u_{3,3}^{(2a)} - \lambda^{(1)}u_{3,3}^{(1a)} \quad , \tag{3}$$

$$P = \beta(u_3^{(2a)} - u_3^{(1a)})/\epsilon^2 + \gamma J_{,3} \quad . \tag{4}$$

The quantities $K^{(\alpha)}$, β and γ in (2)–(4) are mixture properties defined in terms of the fields $v_i^{(\alpha)}$, $w^{*(\alpha)}$ and $w^{(\alpha)}$:

$$K^{(\alpha)} = \frac{\lambda^{(\alpha)}}{A}\oint_{\mathscr{S}} v_i^{(\alpha)}\nu_i^{(1)}\,ds \quad , \tag{5}$$

$$\beta \quad = 1/(w^{*(2a)} - w^{*(1a)}) \quad , \tag{6}$$

$$\gamma \quad = \beta(w^{(1a)} - w^{(2a)}) \quad . \tag{7}$$

The fields $v_i^{(\alpha)}$, $w^{*(\alpha)}$ and $w^{(\alpha)}$, in turn, are solutions of the following micro-structure boundary value problems:

(i) *Plane stress MBVP*

$$\tau_{ij,i}^{(\alpha)} = 0 \qquad \text{on } A^{(\alpha)}, \tag{8}$$

$$\tau_{ij}^{(\alpha)} = \lambda^{(\alpha)}v_{i,i}^{(\alpha)}\delta_{ij} + \mu^{(\alpha)}(v_{i,j}^{(\alpha)} + v_{j,i}^{(\alpha)}), \tag{9}$$

$$v_i^{(2)}\nu_i^{(2)} = 0, \quad \epsilon_{3ij}\tau_{ki}^{(2)}\nu_k^{(2)}\nu_j^{(2)} = 0 \quad \text{on} \quad \mathscr{C}, \tag{10}$$

$$v_i^{(1)} = v_i^{(2)}, \quad (\tau_{ij}^{(2)} - \tau_{ij}^{(1)})\nu_i^{(1)} + \nu_j^{(1)} = 0 \quad \text{on} \quad \mathscr{S}. \tag{11}$$

(ii) *Axial shear MBVP, I*

$$\mu^{(\alpha)} w^{*(\alpha)}_{,i} = \frac{(-1)^{\alpha+1}}{n^{(\alpha)}} \quad \text{on} \quad A^{(\alpha)}, \tag{12}$$

$$w^{*(2)}_{,i} \nu_i^{(2)} = 0 \quad \text{on} \quad \mathscr{C}, \tag{13}$$

$$w^{*(1)} = w^{*(2)}; \quad (\mu^{(1)} w^{*(1)}_{,i} - \mu^{(2)} w^{*(2)}_{,i}) \nu_i^{(1)} = 0, \quad \text{on} \quad \mathscr{S}. \tag{14}$$

(iii) *Axial shear MBVP, II*

$$\mu^{(\alpha)} w^{(\alpha)}_{,ii} = (-1)^{\alpha+1} \frac{K^{(\alpha)}}{n^{(\alpha)}} - (\lambda^{(\alpha)} + \mu^{(\alpha)}) v^{(\alpha)}_{i,i} \quad \text{on} \quad A^{(\alpha)}, \tag{15}$$

$$w^{(2)}_{,i} \nu_i^{(2)} = 0 \quad \text{on} \quad \mathscr{C}, \tag{16}$$

$$w^{(1)} = w^{(2)} \quad \text{on} \quad \mathscr{S}, \tag{17}$$

$$[\mu^{(2)} w^{(2)}_{,i} - \mu^{(1)} w^{(1)}_{,i} + (\mu^{(2)} - \mu^{(1)}) v_i^{(1)}] \nu_i^{(1)} = 0 \quad \text{on} \quad \mathscr{S}. \tag{18}$$

In addition to (12)–(18), $w^{*(\alpha)}$ and $w^{(\alpha)}$ also satisfy conditions for uniqueness:

$$w^{*(1)} = w^{(1)} = 0 \quad \text{at} \quad O \in A^{(1)}. \tag{19}$$

As has been noted in the first part, the Axial Shear MBVP I is exactly the same as the problem encountered in a recent treatment of a similar heat conduction problem[2]. This, of course, is the result of the analogy between anti-plane strain problems and heat conduction in a plane. Since the MBVP for the case of thermal diffusion has been treated in detail in our earlier work[2], only the Plane-Stress MBVP and Axial Shear MBVP II shall be discussed here.

VARIATIONAL PRINCIPLES

In this section, variational principles are proposed in order to develop a finite element procedure for solution of the MBVPs for arbitrary two-dimensional cell geometry. Since it is essential that all the interface conditions be satisfied if the effect of fiber geometry is to be adequately modeled, modified Reissner-type variational principles are utilized. In particular, the variational principle for the plane-stress problem allows the interfacial displacements in the two constituents to have arbitrary variations and the Lagrangian multipliers associated with the jump conditions for the traction vectors turn out to be the components of the average of the interfacial traction vectors in the two constituents. A similar feature is exhibited by the variational principle for the axial shear problem. Thus, in a sense, both the variational principles developed here are of the "mixed" type.

Consider the functional

$$\Pi_1 = \sum_{\alpha=1}^{2} \int\int_{A^{(\alpha)}} \frac{1}{2} \tau_{ij}^{(\alpha)} e_{ij}^{(\alpha)} \, dA + \oint_{\mathscr{S}} (v_i^{(2)} - v_i^{(1)}) T_i \, ds - \frac{1}{2} \oint_{\mathscr{S}} (v_i^{(1)} + v_i^{(2)}) \nu_i^{(1)} \, ds \tag{20}$$

with the kinematic constraint

$$v_i^{(2)} \nu_i^{(2)} = 0 \quad \text{on} \quad \mathscr{C}, \tag{21}$$

and

$$e_{ij}^{(\alpha)} = \frac{1}{2} (v_{i,j}^{(\alpha)} + v_{j,i}^{(\alpha)}). \tag{22}$$

Then, with (9) as additional equations of definition, the condition that Π_1 be stationary with

respect to arbitrary variations in $v_i^{(\alpha)}$ on $A^{(\alpha)}$ and in T_i along $\mathscr{S}$ is equivalent to the problem defined by (8)–(11). To prove this assertion, the first variation of Π_1 is set equal to zero after using the Gauss Theorem to obtain

$$\delta\Pi_1 = -\sum_{\alpha=1}^{2}\int\int_{A^{(\alpha)}} \tau_{ij,i}^{(\alpha)}\delta v_j^{(\alpha)}\,dA + \int_{\mathscr{C}} \tau_{ij}^{(2)}\nu_i^{(2)}\delta v_j^{(2)}\,ds + \oint_{\mathscr{S}}\left[-\tau_{ij}^{(2)}\nu_i^{(1)} + T_j - \frac{\nu_j^{(1)}}{2}\right]\delta v_j^{(2)}\,ds$$

$$+\oint_{\mathscr{S}}\left[\tau_{ij}^{(1)}\nu_i^{(1)} - T_j - \frac{\nu_j^{(1)}}{2}\right]\delta v_j^{(1)}\,ds + \oint_{\mathscr{S}}(v_i^{(2)} - v_i^{(1)})\delta T_i\,ds = 0. \tag{23}$$

Equation (23) implies (8), (11a) and

$$\tau_{ij}^{(2)}\nu_i^{(2)}\delta v_j^{(2)} = 0 \qquad \text{on} \quad \mathscr{C}, \tag{24}$$

$$T_j = \tau_{ij}^{(2)}\nu_i^{(1)} + \frac{\nu_j^{(1)}}{2}$$

$$= \tau_{ij}^{(1)}\nu_i^{(1)} - \frac{\nu_j^{(1)}}{2} \qquad \text{on} \quad \mathscr{S}. \tag{25}$$

From (25) it is easily concluded that the interface condition (11b) is implied by the variational principle and, in addition, the vector T_j represents the average of the interfacial traction vectors in the two constituents. To show that (10b) follows from (24), it is first noted that because of (21), $\delta v_j^{(2)}$ is not arbitrary on $\mathscr{C}$ but can be written as

$$\delta v_j^{(2)} = (\delta_{jk} - \nu_j^{(2)}\nu_k^{(2)})\delta\bar{v}_k \qquad \text{on} \quad \mathscr{C}, \tag{26}$$

where $\delta\bar{v}_k$ is arbitrary. Thus on using (24) and (26), one obtains

$$\tau_{ij}^{(2)}\nu_i^{(2)}(\delta_{jk} - \nu_j^{(2)}\nu_k^{(2)}) = 0 \qquad \text{on} \quad \mathscr{C}. \tag{27}$$

Since $\nu_i^{(2)}$ is a unit vector, the two equations in (27) are linearly dependent and are equivalent to (10b) as can be shown by writing both (27) and (10b) *in extenso*.

The functional appropriate for the axial shear problem (15)–(18) is given by

$$\Pi_3 = \sum_{\alpha=1}^{2}\int\int_{A^{(\alpha)}}\left[\frac{\mu^{(\alpha)}}{2}w_{,j}^{(\alpha)}w_{,j}^{(\alpha)} - (-1)^{\alpha}f^{(\alpha)}w^{(\alpha)}\right]dA + \oint_{\mathscr{S}} Q(w^{(2)} - w^{(1)})\,ds$$

$$-\frac{1}{2}\oint_{\mathscr{S}}(\mu^{(2)} - \mu^{(1)})v_i^{(1)}\nu_i^{(1)}(w^{(1)} + w^{(2)})\,ds \tag{28}$$

with the kinematic constraint (19b) and equation of definition

$$f^{(\alpha)} = \frac{K^{(\alpha)}}{n^{(\alpha)}} + (-1)^{\alpha}(\lambda^{(\alpha)} + \mu^{(\alpha)})v_{i,i}^{(\alpha)}. \tag{29}$$

It is easily shown that the condition that Π_3 be stationary with respect to arbitrary variations in $w^{(\alpha)}$ on $A^{(\alpha)}$ and Q on $\mathscr{S}$ is equivalent to the problem (15)–(18). Indeed,

$$\delta\Pi_3 = -\sum_{\alpha=1}^{2}\int\int_{A^{(\alpha)}}[\mu^{(\alpha)}w_{,jj}^{(\alpha)} + (-1)^{\alpha}f^{(\alpha)}]\delta w^{(\alpha)}\,dA + \oint_{\mathscr{C}}\mu^{(2)}w_{,j}^{(2)}\nu_i^{(2)}\delta w^{(2)}\,ds$$

$$+\oint_{\mathscr{S}}(w^{(2)} - w^{(1)})\delta Q\,ds + \oint_{\mathscr{S}}\left[-\mu^{(2)}w_{,j}^{(2)}\nu_i^{(1)} + Q - \frac{1}{2}(\mu^{(2)} - \mu^{(1)})v_i^{(1)}\nu_i^{(1)}\right]\delta w^{(2)}\,ds$$

$$+\oint_{\mathscr{S}}\left[\mu^{(1)}w_{,j}^{(1)}\nu_i^{(1)} - Q - \frac{1}{2}(\mu^{(2)} - \mu^{(1)})v_i^{(1)}\nu_i^{(1)}\right]\delta w^{(1)}\,ds, \tag{30}$$

so that the equations of the Axial Shear MBVP II are the Euler equations corresponding to the functional Π_3 and, in addition,

$$Q = \frac{1}{2}(\mu^{(1)} w_j^{(1)} + \mu^{(2)} w_j^{(2)}) \nu_j^{(1)}. \tag{31}$$

Thus Q is the average of the interfacial axial shear in the two constituents. The classes of functions over which the extrema of the functionals Π_1 and Π_3 are sought should be such that the first derivatives of the displacements are defined almost everywhere, and the Lagrangian multipliers T_i and Q are piecewise constant on the interface. These conditions, of course, represent the *minimum* degree of continuity required of the shape functions so that all the integrals in (20) and (28) are well defined.

FINITE ELEMENT PROCEDURE

The variational principles developed in the last section can be used to obtain the discrete, finite element analogs of the MBVPs in the usual manner. In the first step towards the completion of this task, the closure of the domains $A^{(1)} \cup A^{(2)}$ is partitioned into closed subdomains $A_{(e)}^{(\alpha)}$, $(e = 1, \ldots N^{(\alpha)})$ where $N^{(\alpha)}$ is the number of elements in $A^{(\alpha)}$. Similarly, the interface $\mathscr{S}$ is partitioned into one-dimensional interface elements $\mathscr{S}_{(e)}$, $(e = 1, \ldots M)$, M being the total number of such elements. In fact, each of the interface elements forms the interelement boundary of two elements $A_{(e)}^{(\alpha)}$, one each in $A^{(1)}$ and in $A^{(2)}$, which overlap at the interface. With this division of the domain of definition of the MBVPs into finite elements, the discretization of the equations proceeds in the following manner.

(i) *Plane stress problem*

The displacement fields $v_i^{(\alpha)}(\mathbf{r})$ are interpolated by the nodal values $u_{2I+i-2}^{(\alpha)} = v_i^{(\alpha)}(\mathbf{r}_I)$ in each finite element $A_{(e)}^{(\alpha)}$ where $\mathbf{r}_I$ is the Ith node of the element. Thus

$$\begin{Bmatrix} v_1^{(\alpha)}(\mathbf{r}) \\ v_2^{(\alpha)}(\mathbf{r}) \end{Bmatrix} = \begin{bmatrix} N_1(\mathbf{r}) & 0 & N_2(\mathbf{r}) & 0 \ \ldots \\ 0 & N_1(\mathbf{r}) & 0 & N_2(\mathbf{r}) \ldots \end{bmatrix} \begin{Bmatrix} u_1 \\ u_2 \\ u_3 \\ \vdots \end{Bmatrix}_{(e)}^{(\alpha)}$$

$$= \mathbf{M}_{(e)} \mathbf{u}_{(e)}^{(\alpha)} \qquad \text{on } A_{(e)}^{(\alpha)} \tag{32}$$

where $N_I(\mathbf{r})$ are interpolation functions used for discretization of the displacement fields on the domain $A_{(e)}^{(\alpha)}$ such that

$$N_I(\mathbf{r}_J) = \delta_{IJ}, \quad \mathbf{r}_J \in A_{(e)}^{(\alpha)}. \tag{33}$$

Similarly, on an interface element $\mathscr{S}_{(e)}$,

$$\begin{Bmatrix} v_1^{(\alpha)}(\mathbf{r}) \\ v_2^{(\alpha)}(\mathbf{r}) \end{Bmatrix} = \begin{bmatrix} \bar{N}_1(\mathbf{r}) & 0 & \bar{N}_2(\mathbf{r}) & 0 \ \ldots \\ 0 & \bar{N}_1(\mathbf{r}) & 0 & \bar{N}_2(\mathbf{r}) \ldots \end{bmatrix} \begin{Bmatrix} \bar{u}_1 \\ \bar{u}_2 \\ \vdots \end{Bmatrix}_{(e)}^{(\alpha)}$$

$$= \bar{\mathbf{M}}_{(e)} \bar{\mathbf{u}}_{(e)}^{(\alpha)}, \tag{34}$$

and

$$\begin{Bmatrix} T_1(\mathbf{r}) \\ T_2(\mathbf{r}) \end{Bmatrix} = \begin{bmatrix} \bar{N}_1(\mathbf{r}) & 0 & \bar{N}_2(\mathbf{r}) & 0 \ \ldots \\ 0 & \bar{N}_1(\mathbf{r}) & 0 & \bar{N}_2(\mathbf{r}) \ldots \end{bmatrix} \begin{Bmatrix} \bar{t}_1 \\ \bar{t}_2 \\ \vdots \end{Bmatrix}_{(e)}$$

$$= \bar{\mathbf{M}}_{(e)} \bar{\mathbf{t}}_{(e)}, \tag{35}$$

where $\bar{N}_I(\mathbf{r})$ are shape functions for interpolation along the interface such that

$$\bar{N}_I(\mathbf{r}_J) = \delta_{IJ}, \quad \mathbf{r}_J \in \mathscr{S}_{(e)}. \tag{36}$$

In (35), the quantities $\bar{t}_{2I+i-2}$ denote the nodal values $T_i(\mathbf{r}_I)$ of the Lagrangian multipliers T_i.

Based on (22) and (32), the vector $\mathbf{e}^{(\alpha)}$ defined by

$$\mathbf{e}^{(\alpha)} = [e_{11}^{(\alpha)}, e_{22}^{(\alpha)}, e_{12}^{(\alpha)}]^T \tag{37}$$

can be written in the form

$$\mathbf{e}^{(\alpha)}(\mathbf{r}) = \mathbf{B}_{(e)}\mathbf{u}_{(e)}^{(\alpha)} \tag{38}$$

where $\mathbf{B}_{(e)}$ is a matrix whose elements are functions of the first derivatives of the interpolation functions $N_I(\mathbf{r})$. The explicit form of the matrix $\mathbf{B}_{(e)}$ can be obtained by using the strain displacement relations, but shall not be given here for the sake of brevity.

Once the field variables have been discretized, the functional Π_1 can be written as

$$\Pi_1 \simeq \sum_{\alpha=1}^{2}\left[\frac{1}{2}\sum_{e=1}^{N^{(\alpha)}}\mathbf{u}_{(e)}^{(\alpha)T}\mathbf{S}_{(e)}^{(\alpha)}\mathbf{u}_{(e)}^{(\alpha)} + \sum_{e=1}^{M}\left\{(-1)^{\alpha}\,\bar{\mathbf{u}}_{(e)}^{(\alpha)T}\mathbf{H}_{(e)}\bar{\mathbf{t}}_{(e)} - \frac{1}{2}\bar{\mathbf{u}}_{(e)}^{(\alpha)T}\mathbf{g}_{(e)}\right\}\right] \tag{39}$$

where

$$\mathbf{S}_{(e)}^{(\alpha)} = \int\int_{A_{(e)}^{(\alpha)}} \mathbf{B}_{(e)}^{T}\mathbf{D}^{(\alpha)}\mathbf{B}_{(e)}\,\mathrm{d}A, \tag{40}$$

$$\mathbf{H}_{(e)} = \oint_{\mathscr{S}_{(e)}} \bar{\mathbf{M}}_{(e)}^{T}\bar{\mathbf{M}}_{(e)}\,\mathrm{d}s, \tag{41}$$

and

$$\mathbf{g}_{(e)} = \oint_{\mathscr{S}_{(e)}} \bar{\mathbf{M}}_{(e)}^{T}\nu^{(1)}\,\mathrm{d}s. \tag{42}$$

In (40), $\mathbf{D}^{(\alpha)}$ is a 3×3 matrix of material constants calculated by using the constitutive relations such that

$$\tau_{ij}^{(\alpha)}e_{ij}^{(\alpha)} = \mathbf{e}^{(\alpha)T}\mathbf{D}^{(\alpha)}\mathbf{e}^{(\alpha)}. \tag{43}$$

Equation (39) can be used together with the usual finite element assembly process to obtain Π_1 in terms of global degrees of freedom. Thus,

$$\Pi_1 \simeq \sum_{\alpha=1}^{2}\left[\frac{1}{2}\mathbf{u}^{(\alpha)T}\mathbf{S}^{(\alpha)}\mathbf{u}^{(\alpha)} + (-1)^{\alpha}\,\bar{\mathbf{u}}^{(\alpha)T}\mathbf{H}\bar{\mathbf{t}} - \frac{1}{2}\bar{\mathbf{u}}^{(\alpha)T}\mathbf{g}\right] \tag{44}$$

where $\mathbf{u}^{(\alpha)}$ is the vector of global degrees of freedom corresponding to $\mathbf{u}_{(e)}^{(\alpha)}$, etc. and it is assumed that during the assembly process the kinematic constraint (21) has been used to eliminate the degrees of freedom which are constrained to be zero. In (44) the vector $\mathbf{u}^{(\alpha)}$ represents the values of the displacements on the nodes lying on the interface as well as on the domain $A^{(\alpha)}$. Thus, without any loss of generality, we can decompose it into the internal nodal displacements $\mathbf{u}^{*(\alpha)}$ and the boundary nodal displacements $\bar{\mathbf{u}}^{(\alpha)}$,

$$\mathbf{u}^{(\alpha)} = \begin{Bmatrix}\mathbf{u}^{*(\alpha)}\\ \bar{\mathbf{u}}^{(\alpha)}\end{Bmatrix}. \tag{45}$$

It is convenient to partition the stiffness matrix $\mathbf{S}^{(\alpha)}$ also in accordance with (45), thus

$$\mathbf{S}^{(\alpha)} = \begin{bmatrix} \mathbf{S}_{11}^{(\alpha)} & \mathbf{S}_{12}^{(\alpha)} \\ \mathbf{S}_{21}^{(\alpha)} & \mathbf{S}_{22}^{(\alpha)} \end{bmatrix}. \tag{46}$$

The discrete analog of the Plane-Stress MBVP can be obtained by extremizing Π_1 with respect to $\mathbf{u}^{(\alpha)}$ and $\bar{\mathbf{t}}$. This leads to

$$\mathbf{S}_{11}^{(\alpha)}\mathbf{u}^{*(\alpha)} + \mathbf{S}_{12}^{(\alpha)}\bar{\mathbf{u}}^{(\alpha)} = 0, \tag{47}$$

$$\mathbf{S}_{21}^{(\alpha)}\mathbf{u}^{*(\alpha)} + \mathbf{S}_{22}^{(\alpha)}\bar{\mathbf{u}}^{(\alpha)} + (-1)^{\alpha}\mathbf{H}\bar{\mathbf{t}} - \frac{1}{2}\mathbf{g} = 0, \tag{48}$$

$$\mathbf{H}(\bar{\mathbf{u}}^{(2)} - \bar{\mathbf{u}}^{(1)}) = 0. \tag{49}$$

Elimination of $\mathbf{u}^{*(\alpha)}$ from (47, 48) results in

$$\mathbf{G}^{(\alpha)}\bar{\mathbf{u}}^{(\alpha)} + (-1)^{\alpha}\mathbf{H}\bar{\mathbf{t}} - \frac{1}{2}\mathbf{g} = 0, \tag{50}$$

where

$$\mathbf{G}^{(\alpha)} = \mathbf{S}_{22}^{(\alpha)} - \mathbf{S}_{21}^{(\alpha)}[\mathbf{S}_{11}^{(\alpha)}]^{-1}\mathbf{S}_{12}^{(\alpha)}. \tag{51}$$

If the interpolation functions are properly chosen, the matrix $\mathbf{H}$ is positive definite, so that from (49) we obtain the continuity of interface displacements,

$$\bar{\mathbf{u}}^{(2)} = \bar{\mathbf{u}}^{(1)}. \tag{52}$$

Equation (52) is now used in (50) and $\bar{\mathbf{t}}$ is eliminated from the two equations implied by the latter. This procedure results in the following expression for the displacements at the interface

$$\bar{\mathbf{u}}^{(1)} = \bar{\mathbf{u}}^{(2)} = [\mathbf{G}^{(1)} + \mathbf{G}^{(2)}]^{-1}\mathbf{g}. \tag{53}$$

Finally, substituting (53) into (47) the displacements at the internal nodes can be computed.

The solution of the plane stress problem can be used to determine the mixture properties $K^{(\alpha)}$ defined by (5) which yields

$$K^{(\alpha)} = \frac{\lambda^{(\alpha)}}{A}\oint_s v_i^{(\alpha)}\nu_i \, ds \simeq \frac{\lambda^{(\alpha)}}{A}\bar{\mathbf{u}}^{(\alpha)T}\mathbf{g}. \tag{54}$$

The solution can also be used to calculate the in-plane dilation which is required for solving the Axial Shear MBVP, II. Thus, at a point $\mathbf{r} \in A_{(e)}^{(\alpha)}$,

$$v_{k,k}^{(\alpha)}(\mathbf{r}) = e_{11}^{(\alpha)} + e_{22}^{(\alpha)} = (1, 1, 0)\mathbf{B}_{(e)}\mathbf{u}_{(e)}^{(\alpha)}. \tag{55}$$

A procedure similar to the one just described can also be used for the solution of the Axial Shear Problem, II. Since the continuity requirements for the shape functions for both problems are the same, identical interpolation functions for discretization of the field variables can be utilized. For this reason, only a brief outline of the computational procedure for the Axial Shear MBVP, II shall be given.

(ii) *Axial shear problem, II*

In terms of local degrees of freedom the discrete analog of the functional Π_3 defined by (28)

is given by

$$\Pi_3 \simeq \sum_{\alpha=1}^{2} \left[\sum_{e=1}^{N^{(\alpha)}} \left\{ \frac{1}{2} \mathbf{q}_{(e)}^{(\alpha)T} \mathbf{K}_{(e)}^{(\alpha)} \mathbf{q}_{(e)}^{(\alpha)} - \mathbf{q}_{(e)}^{(\alpha)T} \mathbf{p}_{(e)}^{(\alpha)} \right\} + \sum_{e=1}^{M} \left\{ (-1)^{\alpha} \bar{\mathbf{q}}_{(e)}^{(\alpha)T} \mathbf{C}_{(e)} \boldsymbol{\psi}_{(e)} - \frac{1}{2} \bar{\mathbf{q}}_{(e)}^{(\alpha)T} \mathbf{h}_{(e)} \right\} \right], \tag{56}$$

where

$$\mathbf{K}_{(e)}^{(\alpha)} = \int\int_{A_{(e)}^{(\alpha)}} \mu^{(\alpha)} \begin{bmatrix} N_{1,1} & N_{1,2} \\ N_{2,1} & N_{2,2} \\ \vdots & \vdots \end{bmatrix} \begin{bmatrix} N_{1,1} & N_{2,1} \dots \\ N_{1,2} & N_{2,2} \dots \end{bmatrix} \mathrm{d}A, \tag{57}$$

$$\mathbf{p}_{(e)}^{(\alpha)} = \int\int_{A_{(e)}^{(\alpha)}} (-1)^{\alpha} \mathbf{N}^T f^{(\alpha)} \, \mathrm{d}A, \tag{58}$$

$$\mathbf{C}_{(e)} = \oint_{\mathcal{S}_{(e)}} \bar{\mathbf{N}}^T \bar{\mathbf{N}} \, \mathrm{d}s, \tag{59}$$

$$\mathbf{h}_{(e)} = \oint_{\mathcal{S}_{(e)}} (\mu^{(2)} - \mu^{(1)}) \bar{\mathbf{N}}^T v_i^{(1)} \nu_i^{(1)} \, \mathrm{d}s. \tag{60}$$

In (56) $\mathbf{q}_{(e)}^{(\alpha)}$ represents the nodal values of the field $w^{(\alpha)}$, and $\boldsymbol{\psi}_{(e)}$ denotes the Lagrangian multipliers Q at the interface nodes. The matrices $\mathbf{N}$ and $\bar{\mathbf{N}}$ are defined in terms of interpolation functions, thus

$$\mathbf{N} = [N_1(\mathbf{r}), \quad N_2(\mathbf{r}) \dots] \qquad \text{on } A_{(e)}^{(\alpha)}, \tag{61}$$

$$\bar{\mathbf{N}} = [\bar{N}_1(\mathbf{r}), \quad \bar{N}_2(\mathbf{r}) \dots] \qquad \text{on } \mathcal{S}_{(e)}, \tag{62}$$

Using the finite element assembly process after elimination of the degree of freedom constrained by the kinematic condition (19), we obtain the functional Π_3 in terms of global degrees of freedom in the form

$$\Pi_3 \simeq \sum_{\alpha=1}^{2} \left[\frac{1}{2} \mathbf{q}^{(\alpha)T} \mathbf{K}^{(\alpha)} \mathbf{q}^{(\alpha)} - \mathbf{q}^{(\alpha)T} \mathbf{p}^{(\alpha)} + (-1)^{\alpha} \bar{\mathbf{q}}^{(\alpha)T} \mathbf{C} \boldsymbol{\Psi} - \frac{1}{2} \bar{\mathbf{q}}^{(\alpha)T} \mathbf{h} \right]. \tag{63}$$

Extremization of Π_3 with respect to $\mathbf{q}^{(\alpha)}$ and $\boldsymbol{\Psi}$ leads to the following discrete version of the axial shear problem:

$$\mathbf{K}_{11}^{(\alpha)} \mathbf{q}^{*(\alpha)} + \mathbf{K}_{12}^{(\alpha)} \bar{\mathbf{q}}^{(\alpha)} - \mathbf{p}^{*(\alpha)} = 0, \tag{64}$$

$$\mathbf{K}_{21}^{(\alpha)} \mathbf{q}^{*(\alpha)} + \mathbf{K}_{22}^{(\alpha)} \bar{\mathbf{q}}^{(\alpha)} - \bar{\mathbf{p}}^{(\alpha)} + (-1)^{\alpha} \mathbf{C} \boldsymbol{\Psi} - \frac{1}{2} \mathbf{h} = 0, \tag{65}$$

$$\mathbf{C}(\bar{\mathbf{q}}^{(2)} - \bar{\mathbf{q}}^{(1)}) = 0, \tag{66}$$

where the partition analogous to (45) has been made for $\mathbf{p}^{(\alpha)}$. The set (64–66) can be solved by first eliminating the internal nodal quantities $\mathbf{q}^{*(\alpha)}$. The result of this procedure is

$$\bar{\mathbf{q}}^{(1)} = \bar{\mathbf{q}}^{(2)} \simeq [\mathbf{F}^{(1)} + \mathbf{F}^{(2)}]^{-1} \left\{ \bar{\mathbf{h}} - \sum_{\alpha=1}^{2} \mathbf{K}_{21}^{(\alpha)} [\mathbf{K}_{11}^{(\alpha)}]^{-1} \mathbf{p}^{(\alpha)} \right\} \tag{67}$$

where

$$\mathbf{F}^{(\alpha)} = \mathbf{K}_{22}^{(\alpha)} - \mathbf{K}_{21}^{(\alpha)}[\mathbf{K}_{11}^{(\alpha)}]^{-1}\mathbf{K}_{12}^{(\alpha)}, \tag{68a}$$

$$\bar{\mathbf{h}} = \mathbf{h} + \bar{\mathbf{p}}^{(1)} + \bar{\mathbf{p}}^{(2)}. \tag{68b}$$

Finally, (64) can be used to calculate the internal nodal quantities. Once the field $w^{(\alpha)}$ has thus been determined it is a simple matter to calculate the mixture property γ from (7) since the averages

$$w^{(\alpha a)} = \frac{1}{A^{(\alpha)}} \int\int_{A^{(\alpha)}} w^{(\alpha)} \, dA \tag{69}$$

can be evaluated by numerical integration.

NUMERICAL RESULTS FOR MIXTURE PROPERTIES

The computational procedure described in the preceding section has been used to calculate mixture properties for several microstructural geometries and combinations of material properties. Six node conforming triangular elements were used for discretization of the displacement fields within each constituent, and for the interface quantities compatible quadratic interpolation functions were utilized.

The mixture properties $K^{(\alpha)}$ determine the mixture modulus $E_{(m)}$ of the composite in the direction of the fiber axis. The variation of mixture moduli for composites containing circular fibers in a hexagonal array has been depicted in Fig. 1. This figure also shows the mixture moduli calculated by approximating the cell by a circular cylinder. It is evident that the approximation is very accurate and it is not necessary to numerically solve the Plane Stress MBVP if the only desired quantity is the mixture modulus. Some conclusion can be drawn from Fig. 2 for composites containing rectangular fibers in a similar unit cell. Similar calculations for different aspect ratios of the unit cell have indicated that the geometry of the fiber and the unit cell has very little effect on mixture moduli.

In Figs. 3–6, we have shown the interaction coefficients β and γ [see eqn 4]. Again the axisymmetric approximation is seen to be adequate for calculating these mixture properties. For rectangular fibers arranged in similar unit cells, however, the accuracy of the approximation is not satisfactory. This conclusion can be drawn from Figs. 7–10 which show the variation of the interaction coefficients for different aspect ratios of the unit cell. Moreover, if the aspect ratio is not close to unity, it is imperative that the MBVPs be solved numerically if the analysis is to take adequate account of the fiber and the cell geometry.

APPLICATION: DISPERSION OF LONGITUDINAL WAVES

The material properties determined for various composites have been used to study the dispersion of time-harmonic waves for many microstructural geometries and material properties combinations. Consider time harmonic waves of the form

$$u_3^{(\alpha a)}(x_3, t) = \Phi_\alpha e^{i(kx_3 - \omega t)} \tag{70}$$

propagating in the direction of the fiber axis. If (70) is substituted into (1) and the condition for the existence of a nontrivial solution is imposed, the following dispersion relation between the phase velocity $c_p = \omega/k$ and frequency ω can be derived:

$$\epsilon\omega = c_p\left[\frac{\bar{\beta}(c_p^2 - 1)}{(c_+^2 - c_p^2)(c_-^2 - c_p^2)}\right]^{1/2}. \tag{71}$$

The constants in (71) are given by

$$\bar{\beta} = \beta/(\rho^{(1p)}\rho^{(2p)}), \tag{72a}$$

$$c_\pm^2 = [c_1^2 + c_2^2 \pm \sqrt{((c_1^2 - c_2^2)^2 + 4c_3^4)}]/2 \tag{72b}$$

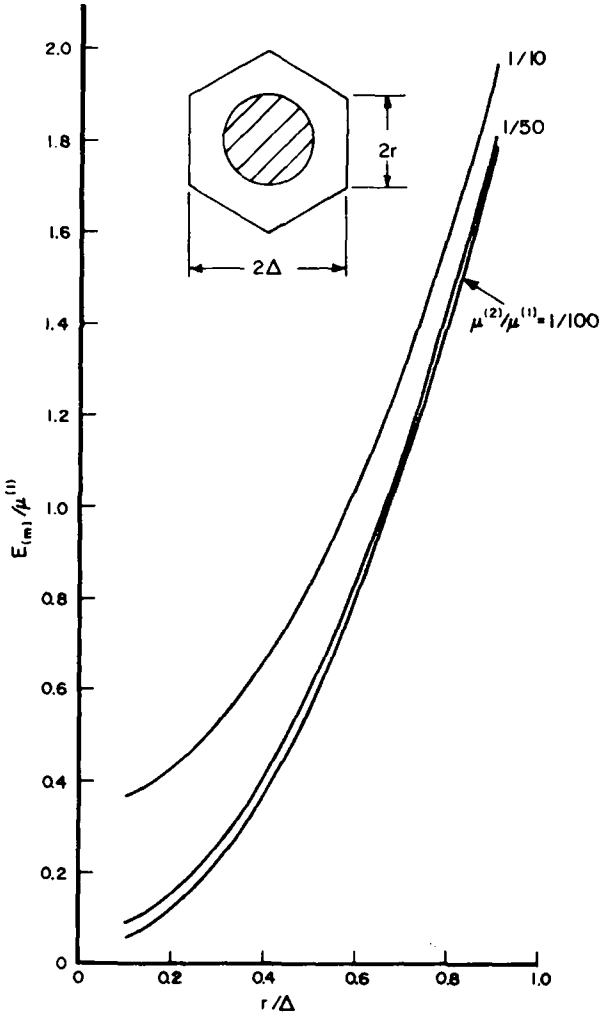

Fig. 1. Mixture modulus for composites containing circular fibers in hexagonal array: finite element solution and axisymmetric approximation.

where

$$c_\alpha^2 = [\lambda^{(\alpha p)} + 2\mu^{(\alpha p)} - (K^{(\alpha)} + \gamma)\lambda^{(\alpha)}]/\rho^{(\alpha p)}, \tag{73a}$$

$$c_3^4 = [(K^{(1)} + \gamma)(K^{(2)} + \gamma)\lambda^{(1)}\lambda^{(2)}]/[\rho^{(1p)}\rho^{(2p)}]. \tag{73b}$$

A detailed discussion of the qualitative nature of the dispersion relation (71) has been given by Hegemier *et al.*[3].

Using the mixture properties $K^{(\alpha)}$, β and γ presented in the previous section, dispersion curves have been obtained for composites with circular fibers in hexagonal cells and with rectangular fibers in similar rectangular cells of different slenderness ratio. In all the computations the ratio of fiber and matrix densities was taken to be 1.75 (Table 1), a number typical of many composites.

In Figs. 11–14, the effect of changing the fiber volume fraction on the phase velocity spectra has been shown for the same fiber and matrix material combinations. The curves show that as the fiber volume fraction is increased, the phase velocity spectrum tends to flatten out in the low frequency region, i.e. the composite tends to be less dispersive. This is not unexpected, since in the limit as fiber volume fraction approaches unity, the theory should predict nondispersive behavior.

Figures 15–18 depict the effect of changing the stiffness ratio. Again, the correct qualitative

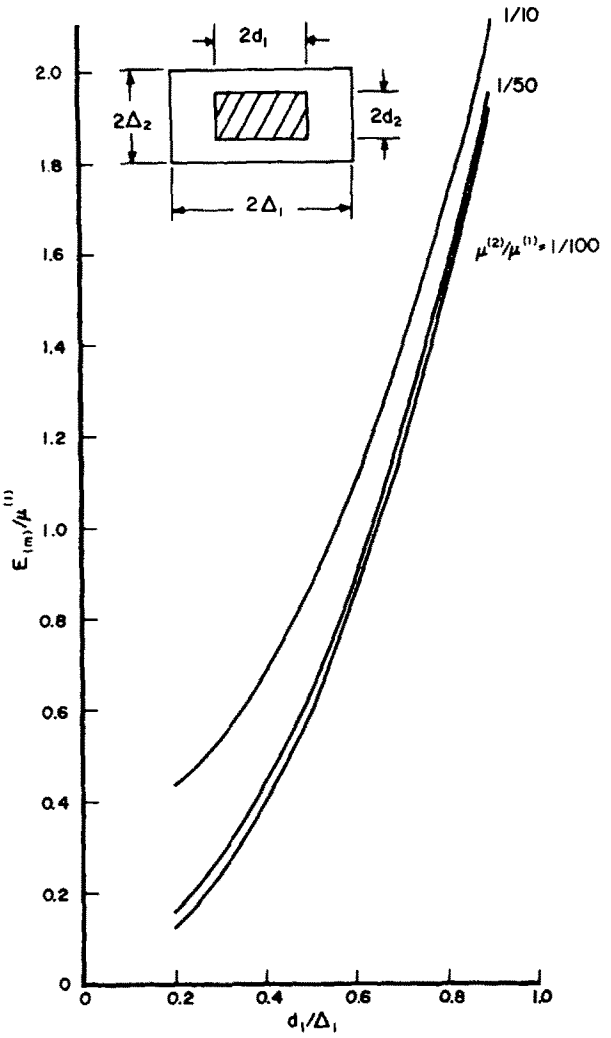

Fig. 2. Mixture modulus for composites containing rectangular fibers in similar unit cells (aspect ratio: $\Delta_1/\Delta_2 = d_1/d_2 = 2$): finite element solution and axisymmetric approximation.

Table 1. Composite parameters used for comparison with experimental data

A. Cell Dimensions: $R_2 = 2.722$, $R_1 = 2.0(\times 10^{-3}$ in)

B. Material Properties

	Boron	Epoxy
Volume fraction (%)	54*	46
Young's modulus in fibre direction (10^6 psi)	55.0	0.73
Poisson's ratio	0.20	0.31
Density $10^{-6}\frac{lb_f\ sec^2}{in^4}$	251	118

behavior is observed, inasmuch as the dispersion becomes more pronounced as the stiffness of the fiber becomes much larger than that of the matrix. In these figures (eqns 15–18), the dispersion curves for the hexagonal and rectangular cells have also been compared with the phase velocity spectra obtained by using concentric circular cylinders approximation for which the MBVPs can be solved analytically[3, 4]. It can be observed that the concentric cylinders

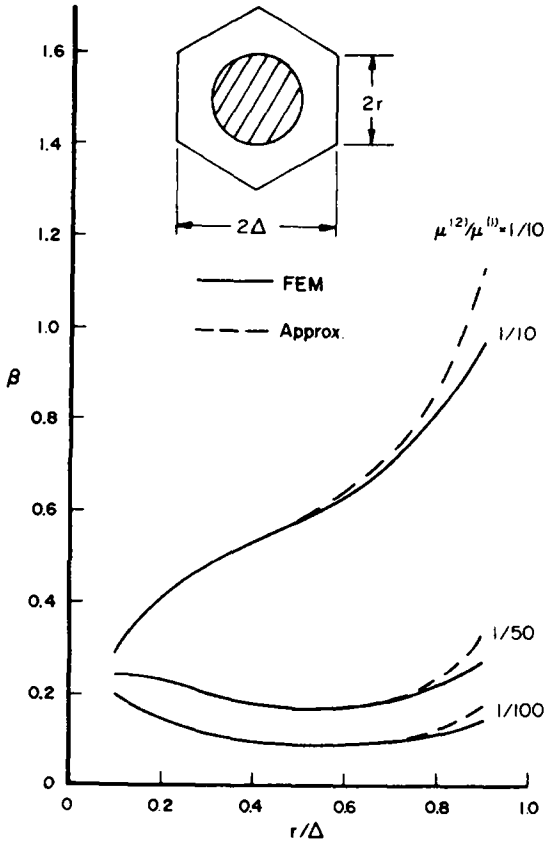

Fig. 3. Interaction coefficient β for composites containing circular fibers in hexagonal array.

approximation gives excellent agreement with the elaborate results of the mixture theory based on the FEM analysis for hexagonal and square cells. However, for cells with slenderness ratio different from unity, the approximation just mentioned is not adequate and, for this reason, a computational approach to the solution of the MBVPs becomes a necessity.

COMPARISON WITH EXPERIMENTAL DATA

In order to demonstrate the efficacy of the proposed model, in this section, we compare the mixture theory predictions on dispersion of longitudinal waves in a boron/epoxy fiber reinforced composite with the experimental data reported by Tauchert and Guzelsu[3]. The data was acquired by using ultrasonic techniques to measure group velocity as a function of frequency of harmonic waves propagating in a specimen containing circular fibers arranged in a square array.

Based on the numerical results presented in the last section which indicated that the concentric circular cylindrical approximation is adequate for composites containing square fibers in a similar unit cell (see Fig. 16), we use the axisymmetric approximation for the microstructural geometry used by Tauchert and Guzelsu[3]. Using the results of a parallel study[4], wherein the details of the solution for the concentric cylinders approximation have been presented, we have

$$K^{(\alpha)} = \lambda^{(\alpha)}/E_0 \tag{74a}$$

$$\beta = 8/\left\{\frac{1}{\mu^{(1)}} - \frac{1}{n^{(2)}\mu^{(2)}}\left(2 + n^{(2)} + \frac{2\ln n^{(1)}}{n^{(2)}}\right)\right\} \tag{74b}$$

$$\gamma = \frac{-1}{4E_0 n^{(2)}}\left(1 + \frac{\ln n^{(1)}}{n^{(2)}}\right)\beta \tag{74c}$$

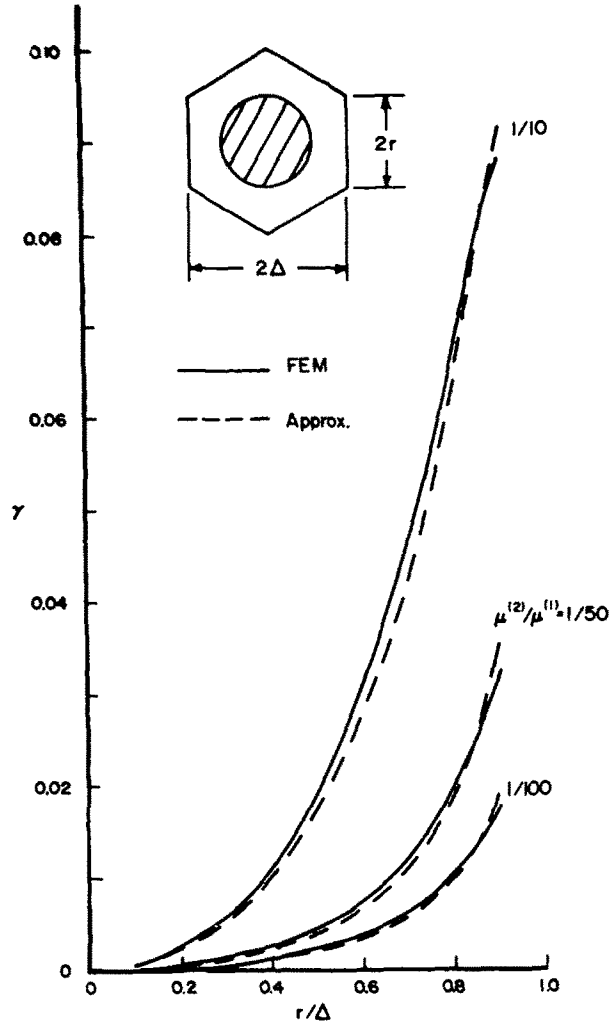

Fig. 4. Interaction coefficient γ for composites containing circular fibers in hexagonal array.

where

$$E_0 = \frac{n^{(2)}(\lambda+\mu)^{(1)} + n^{(1)}(\lambda+\mu)^{(2)} + \mu^{(2)}}{n^{(1)}n^{(2)}}. \tag{74d}$$

The material properties used for (74) are given in Table 1, which also shows the dimensions of the concentric circular cylinders based on equal volume fractions.

Substitution of (70) into (1) yields the following characteristic equation:

$$\alpha\{k^2(C_{11}+C_{22}+2C_{12}) - (\rho^{(1p)}+\rho^{(2p)})\omega^2\} + \epsilon^2 k^4\{(C_{11}-\xi_1)(C_{22}-\xi_2) - (C_{12}+\xi_1)(C_{12}+\xi_2)\}$$

$$-\epsilon^2 k^2\omega^2\{\rho^{(1p)}(C_{22}-\xi_2) + \rho^{(2p)}(C_{11}-\xi_1)\} + \epsilon^2\omega^4\rho^{(1p)}\rho^{(2p)} = 0 \tag{75}$$

where

$$C_{11} = n^{(1)}(\lambda+2\mu)^{(1)} - \frac{\lambda^{(1)2}}{E_0}, \tag{76a}$$

$$C_{22} = n^{(2)}(\lambda+2\mu)^{(2)} - \frac{\lambda^{(2)2}}{E_0}, \tag{76b}$$

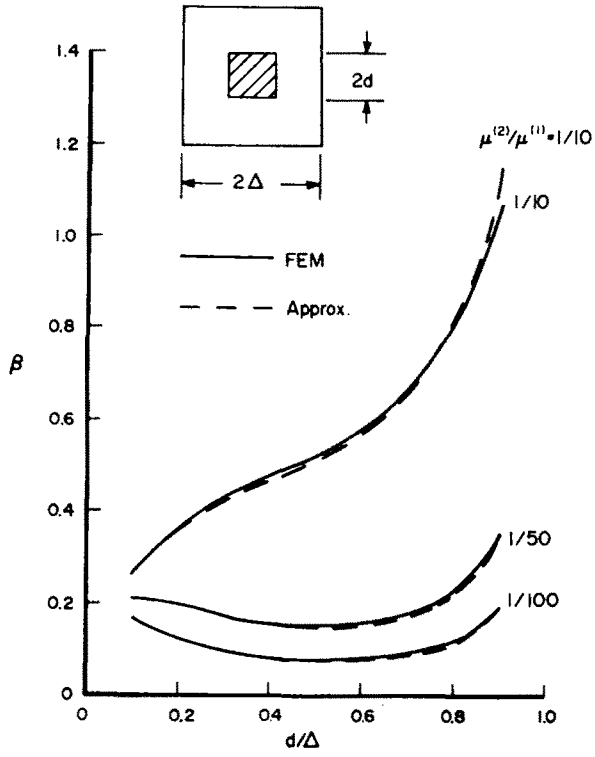

Fig. 5 Interaction coefficient β for composites containing square fibers in similar unit cells.

$$C_{12} = \frac{\lambda^{(1)}\lambda^{(2)}}{E_0}, \quad \xi_\alpha = \lambda^{(\alpha)}\gamma. \tag{76c}$$

From (75) phase velocity $C_p = (\omega/k)$ and group velocity $C_g = (\mathrm{d}\omega/\mathrm{d}k)$ are easily obtained for each $\epsilon\omega$. In order to recover dimensional quantities, we first calculate $\bar{E}_{(m)}$ and $\bar{\rho}_{(m)}$ from (65) of [1] and obtain

$$\bar{c}_{(m)} = \sqrt{(\bar{E}_{(m)}/\bar{\rho}_{(m)})} = 0.4 \times 10^6 \text{ in/sec}. \tag{77}$$

From the scaling in[1], we have

$$\epsilon\omega = \frac{\bar{R}_2}{\bar{\Lambda}} \bar{t}_0 2\pi\nu = \frac{\bar{R}_2}{\bar{\Lambda}} \frac{\bar{\Lambda}}{\bar{c}_{(m)}} 2\pi\nu. \tag{78a}$$

As a result, dimensional frequency is obtained as follows:

$$\nu = \frac{\bar{c}_{(m)}}{2\pi\bar{R}_2} \cdot \epsilon\omega = 23.39 \times 10^6 \cdot \epsilon\omega \text{ cps}. \tag{78b}$$

The group velocity spectrum obtained from (75) is shown in Fig. 19 together with the experimental data. Even though this application is only a special case of our treatment for arbitrary fibers, the close agreement of the results of the mixture theory with the experimental data establishes the validity of our approach.

CONCLUDING REMARKS

A computational procedure has been presented for solution of the microstructure boundary value problems derived in the first part of the paper. The procedure can be used to calculate the mixture properties that are required for solution of the mixture equations for longitudinal wave propagation in fibrous composites. The technique is applicable to the composites containing fibers of arbitrary cross section arranged in a general two-dimensional array.

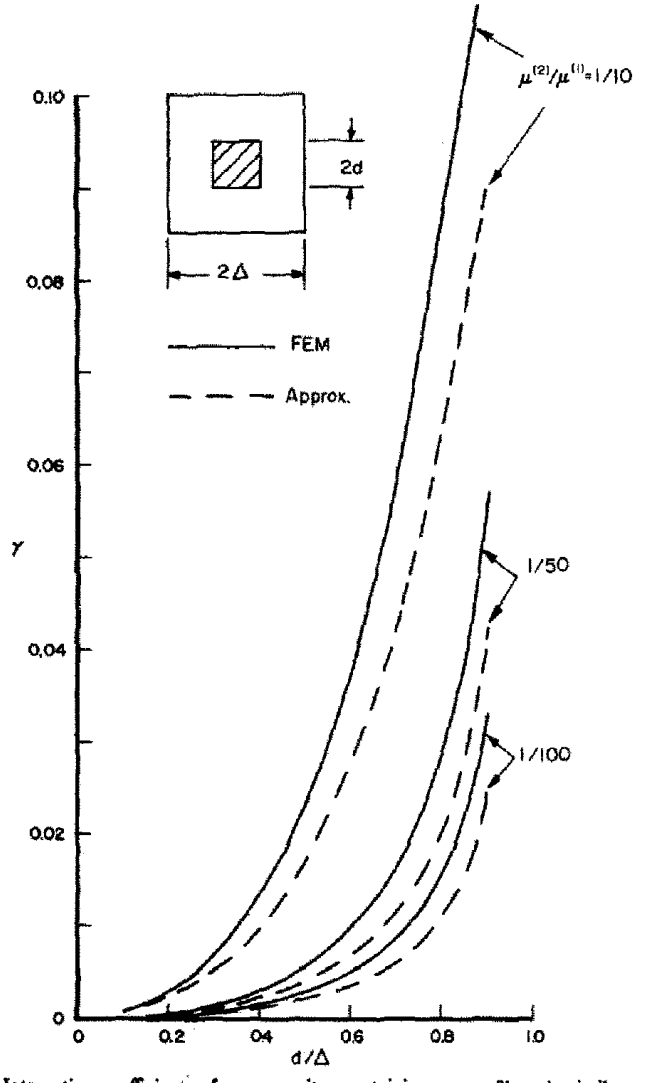

Fig. 6. Interaction coefficient γ for composites containing square fibers in similar unit cells.

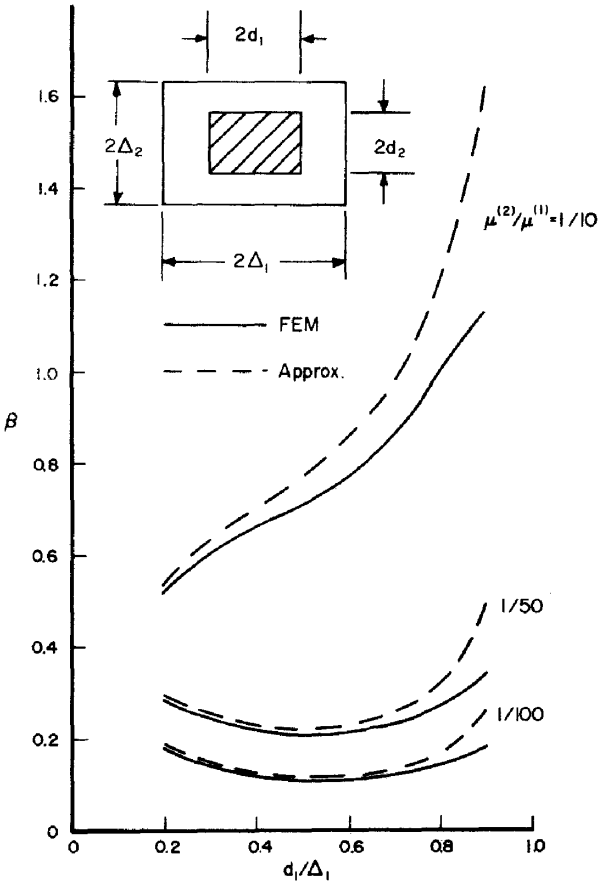

Fig. 7. Interaction coefficient β for composites containing rectangular fibers in similar unit cells (aspect ratio: $\Delta_1/\Delta_2 = 1.5$).

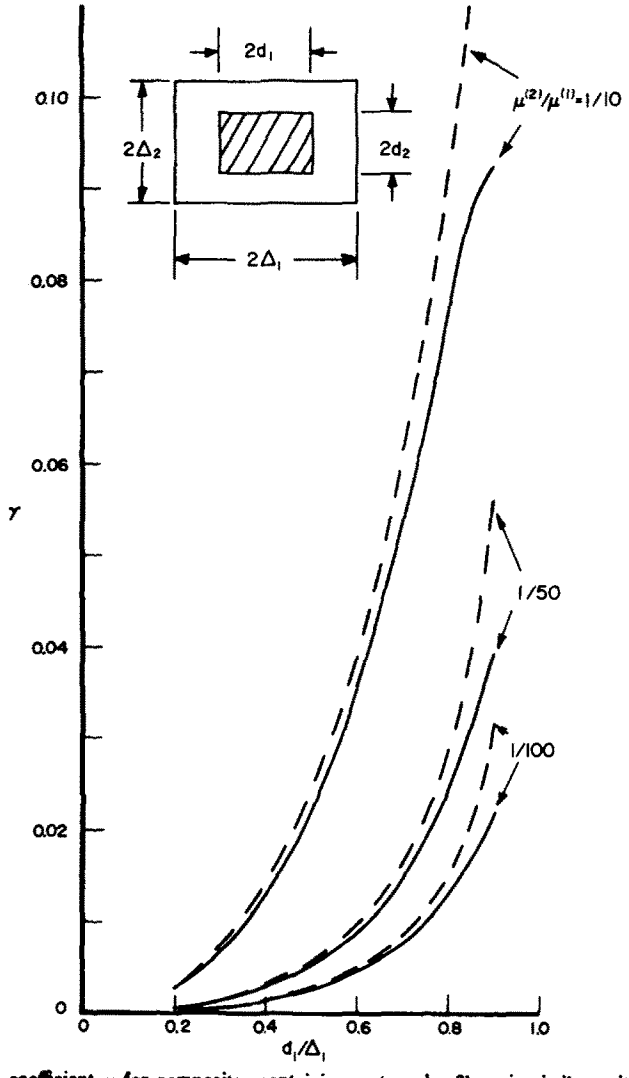

eraction coefficient γ for composites containing rectangular fibers in similar unit cells (aspect ratio: $\Delta_1/\Delta_2 = 1.5$).

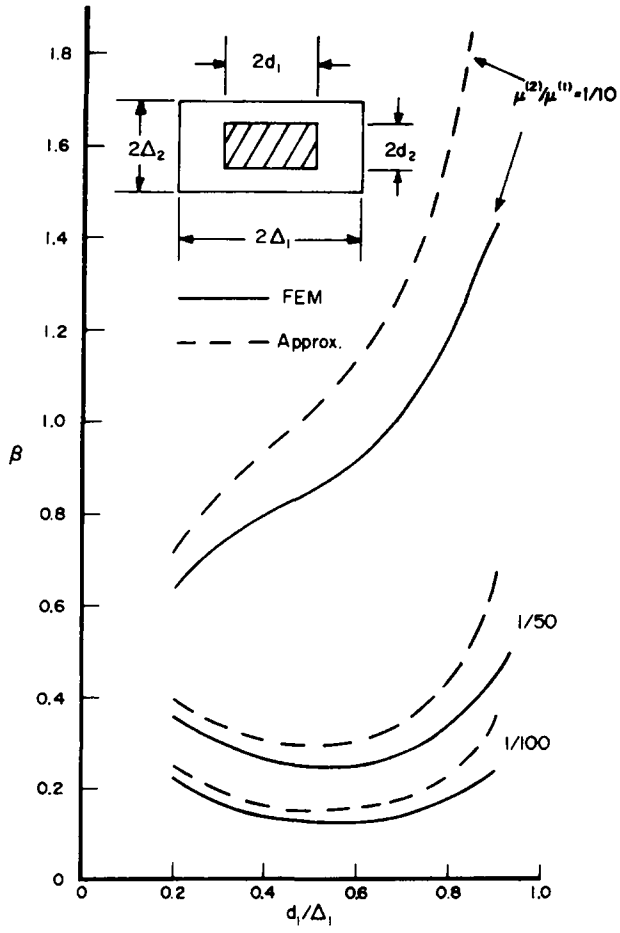

Fig. 9. Interaction coefficient β for composites containing rectangular fibers in similar unit cells (aspect ratio: $\Delta_1/\Delta_2 = 2$).

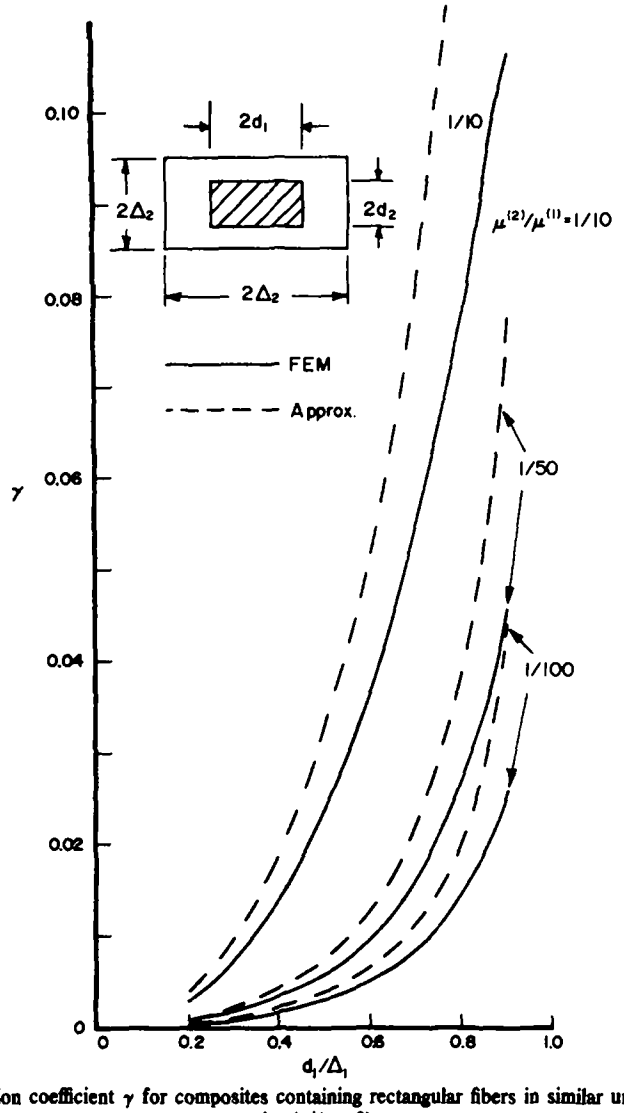

Fig. 10. Interaction coefficient γ for composites containing rectangular fibers in similar unit cells (aspect ratio: $\Delta_1/\Delta_2 = 2$).

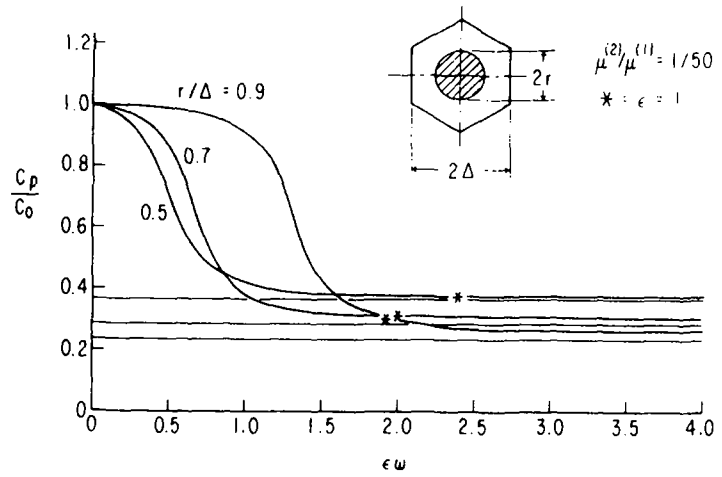

Fig. 11. Phase velocity spectrum for a composite containing circular fibers in hexagonal array-effect of changing the fiber volume fraction.

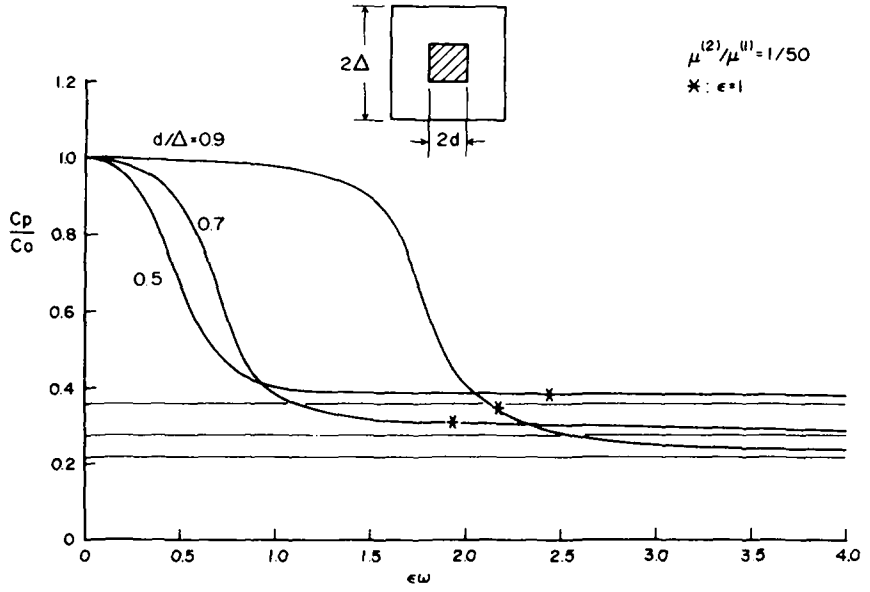

Fig. 12. Phase velocity spectrum for a composite containing square fibers in square array-effect of changing the fiber volume fraction.

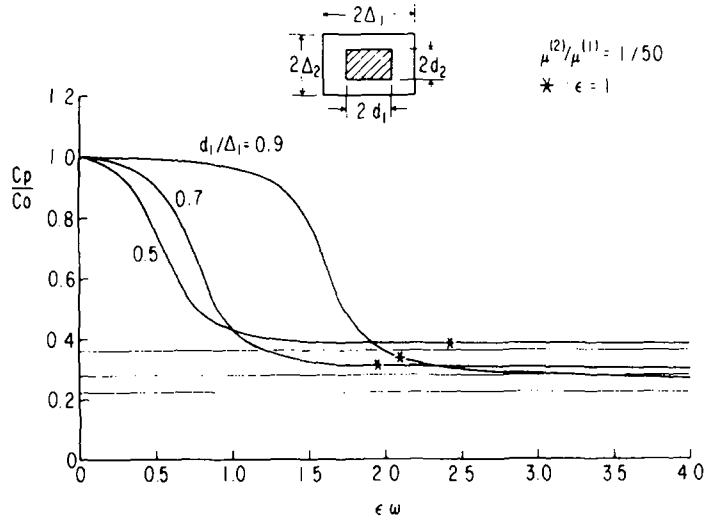

Fig. 13. Phase velocity spectrum for a composite containing rectangular fibers in similar unit cells ($\Delta_1/\Delta_2 = 1.5$)—effect of changing the fiber volume fraction.

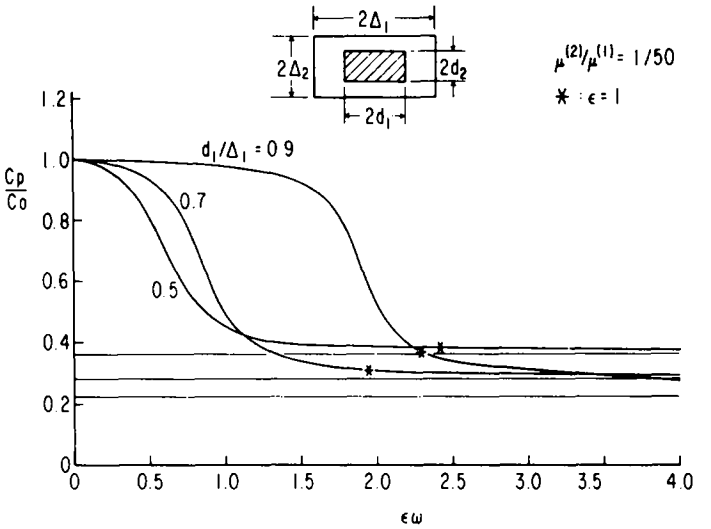

Fig. 14. Phase velocity spectrum for a composite containing rectangular fibers in similar unit cells ($\Delta_1/\Delta_2 = 2$)—effect of changing the fiber volume fraction.

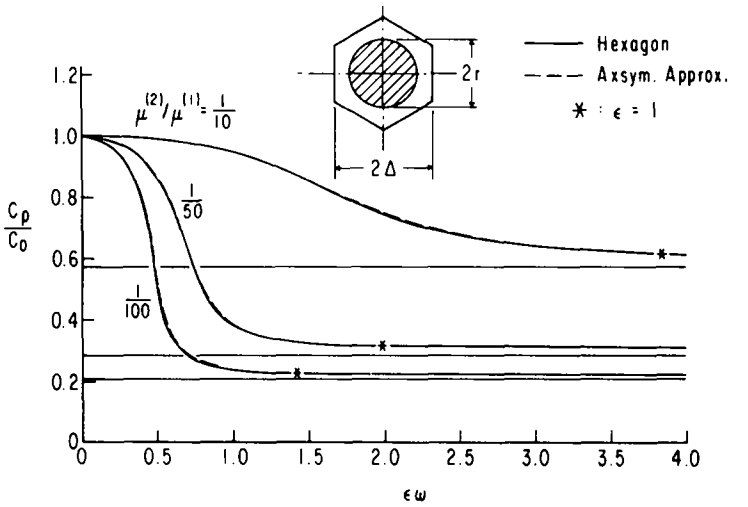

Fig. 15. Phase velocity spectrum for a composite containing circular fibers in a hexagonal array—effect of changing the stiffness ratio $r/\Delta = 0.7$.

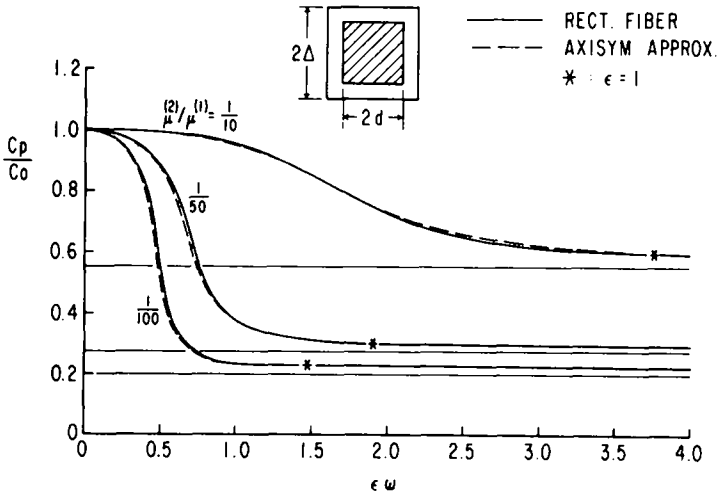

Fig. 16. Phase velocity spectrum for a composite containing square fibers in a square array—effect of changing the stiffness ratio ($d_1/\Delta_1 = 0.7$).

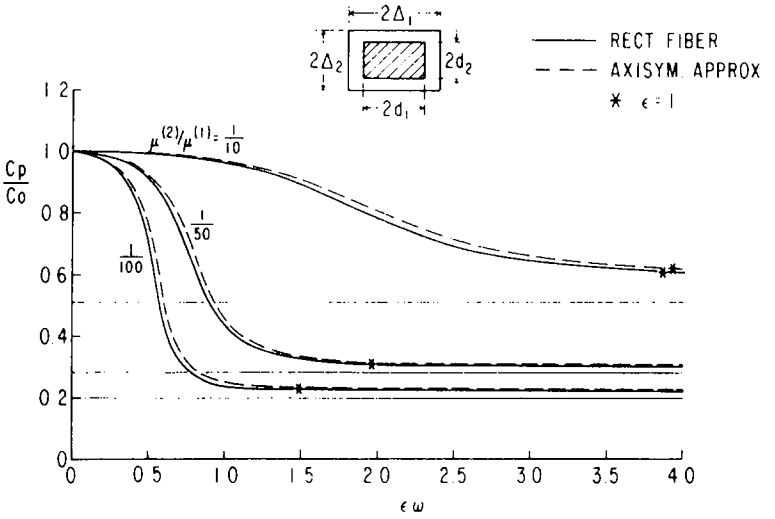

Fig. 17. Phase velocity spectrum for a composite containing rectangular fibers in a similar unit cells ($\Delta_1/\Delta_2 = 1.5$)—effect of changing the stiffness ratio ($d_1/\Delta_1 = 0.7$).

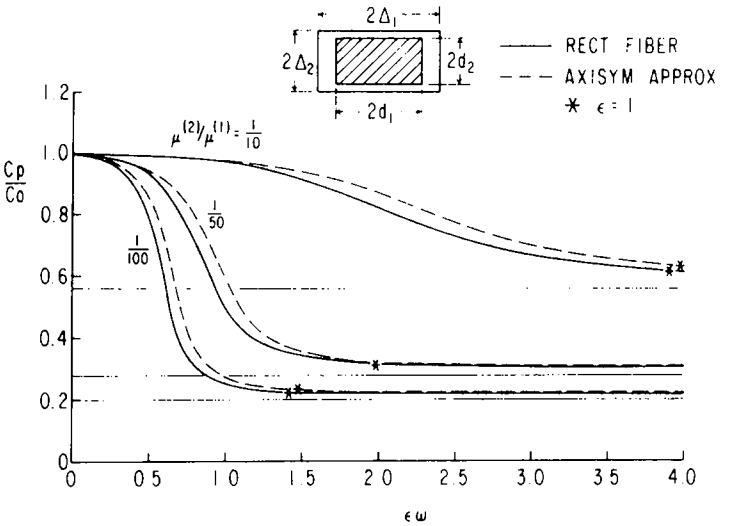

Fig. 18. Phase velocity spectrum for a composite containing rectangular fibers in similar unit cells ($\Delta_1/\Delta_2 = 2$)—effect of changing the stiffness ratio ($d_1/\Delta_1 = 0.7$).

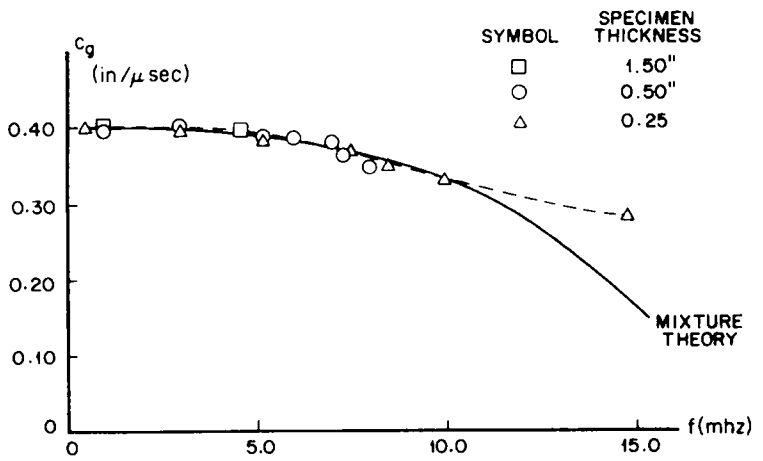

Fig. 19. Comparison with experimental data: Group velocity vs frequency for boron/epoxy composite (see [4]).

Numerical results indicate that for the calculation of the mixture modulus in the direction of the fiber axis, the shape of the fiber cross section is not very important and one can use the concentric circular cylinders approximation without any significant loss of accuracy. For composites containing circular fibers in a hexagonal array, the approximation is adequate for determination of other mixture properties also. Although such a conclusion appears to be intuitively obvious, the fact that our numerical analysis also confirms it bears out the soundness of our approach.

For computation of interaction coefficients for composites containing noncircular fibers, the procedure described here appears to be a necessity. However, since the technique requires the solution of time independent problems in a two-dimensional domain, our methodology is quite attractive from the point of view of computational efficiency.

Application of the mixture theory to dispersion of time harmonic waves indicates the range of parameters in which it may not be appropriate to model the unit cell and fiber by concentric circular cylinders.

REFERENCES

1. H. Murakami, A. Maewal and G. A. Hegemier, Mixture theory for longitudinal wave propagation in unidirectional composites with cylinder fibers of arbitrary cross section—I. Formulation. *Int. J. Solids Structures* **15**, 325–334 (1979).
2. H. Murakami, G. A. Hegemier and A. Maewal, Mixture theory for thermal diffusion in unidirectional composites with fibers of arbitrary cross-section. *Int. J. Solids Structures* **14**, 723–737 (1978).
3. T. R. Tauchert and A. N. Guzelsu, An experimental study of dispersion of stress waves in a fiber reinforced composite. *J. Appl. Mech.* **39**, 98 (1974).
4. A. Maewal, H. Murakami and G. A. Hegemier, Effect of constituent anisotropy on longitudinal wave propagation in fibrous composites. To be published.